Rare Metal Materials and Engineering
Volume 41, Issue 9, September 2012
Online English edition of the Chinese language journal

Cite this article as: Rare Metal Materials and Engineering, 2012, 41(9): 1505-1510.

ARTICLE

Effects of Diamond-like Carbon Coatings with Different Thickness on Mechanical Properties and Corrosion Behavior of Biomedical NiTi Alloy

Hang Ruiqiang[1], Ma Shengli[1], Chu K. Paul[2]

[1] State Key Laboratory for Mechanical Behavior of Materials, Xi'an Jiaotong University, Xi'an 710049, China; [2] City University of Hong Kong, Kowloon, Hong Kong, China

Abstract: Diamond-like carbon (DLC) coatings with the thickness between 253-1880 nm were prepared on NiTi alloy by arc enhanced magnetron sputtering (AEMS). Surface profilometry, scratch tests, tribometry, and electrochemical tests were conducted to determine the mechanical properties and the corrosion behavior of the DLC-coated NiTi alloy, and it is found that DLC coatings with thickness between 700 and 1000 nm have moderate residual stress, high critical load, long wear life and good corrosion resistance. So DLC coatings with thickness between 700 and 1000 nm are suitable for improving the mechanical properties and corrosion resistance of biomedical NiTi alloy. The associated mechanisms were also discussed in detail.

Key words: diamond-like carbon; nickel-titanium; mechanical property; corrosion behavior

Nearly equiatomic nickel-titanium (NiTi) shape memory alloy is promising in biomedical implants for orthopedics and cardiovascular surgery because of its distinctive shape memory effect and super-elasticity that other metallic implants do not possess[1,2]. However, the high Ni content is a potential health concern because after introduction into human body, the Ni ions will leach from the bulk materials into surrounding tissues in spontaneous electrochemical corrosion processes. A study of the cytotoxicity of Ni based on gene expression profiles shows that Ni ions can inhibit the proliferation and differentiation of mouse fibroblast cells (L-929) by changing the expression level of related genes[3]. It has also been reported that Ni ions can cause allergic reactions especially in Ni hyper-sensitive patients[4]. Fretting on orthopedic implants occurs frequently[1] and fretting wear at the articulating surface can expedite release of toxic Ni ions[5]. Hence, it is important to enhance the surface properties such as anti-wear properties and corrosion resistance of the materials before they can be safely used clinically.

Diamond-like carbon (DLC) coatings are promising materials in the surface modification of biomedical NiTi alloy because of their excellent properties such as low friction coefficient, biocompatibility, good corrosion resistance and anti-wear properties[6]. Many researchers have deposited DLC coatings on NiTi alloy using different techniques. S. Kobayashi, et al deposited DLC coatings with about 1 μm thickness on NiTi alloy using ion beam plating and found the improved wear performance and corrosion resistance[7]. J.H. Sui, et al used plasma immersion ion implantation and deposition (PIII&D) to fabricate DLC coatings with about 600 nm thickness on NiTi alloy using various pressure and bias voltage settings and found that an increased working pressure decreased the corrosion resistance[8] whereas a higher bias voltage first increased the corrosion resistance and then decreased it[9]. Y.F. Zheng, et al deposited DLC coatings with 350-500 nm thickness on NiTi alloy by PIII&D in conjunction with plasma enhanced chemical vapor deposition (PECVD) using different bias voltages and observed that the corrosion resistance increased initially and then decreased with increasing of bias voltage[10]. It is known that the film thickness has a significant

Received date: September 10, 2011
Foundation item: Joint Project of Guangdong Province and Ministry of Education of China (2007A090302087); City University of Hong Kong Applied Research Grant (ARG) (9667028)
Corresponding author: Hang Ruiqiang, Candidate for Ph. D., State Key Laboratory for Mechanical Behavior of Materials, Xi'an Jiaotong University, Xi'an 710049, Tel: 0086-29-82668395, E-mail: r.q.hang@stu.xjtu.edu.cn; Ma Shengli, Professor, E-mail: slma@mail.xjtu.edu.cn

influence on the wear life, adhesion as well as corrosion resistance of coatings but the associated work and reports about DLC coatings on NiTi alloy have been just few. The purpose of this study is to investigate the effects of coating thickness on the mechanical properties and corrosion behavior of DLC-coated NiTi alloy prepared by arc enhanced magnetron sputtering (AEMS).

1 Experiment

1.1 Coating deposition and characterization

P-type silicon wafers (100) and mirror polished NiTi (50.7 at.%Ni) alloy were used as substrates. Arch enhanced magnetron sputtering (AEMS) was used to deposit DLC coatings. The deposition process was referred in our previously study[11] and the deposition time was 15, 30, 60, 90, 120, 150 and 180 min, respectively. Raman spectroscopy (ALMEGA, USA) was used to determine the chemical structure of the DLC coatings using the Ar laser with excitation wavelength of 532 nm and power of 25 mW. The film thickness was observed by field-emission scanning electron spectroscopy (FE-SEM, JSM-7000F) at an accelerating voltage of 20 kV. Three different regions were measured to obtain an average film thickness.

1.2 Mechanical properties

The residual stress σ_s in the DLC coatings (σ_s) was calculated using Stoney's equation[12]:

$$\sigma_s = \frac{E_s}{6(1-\upsilon_s)} \frac{t_s^2}{t_c} \left(\frac{1}{R} - \frac{1}{R_0} \right) \quad (1)$$

Where E_s, t_s and υ_s are the Young's modulus, thickness, and Poisson's ratio of the silicon wafer, t_c is the film thickness, and R and R_0 are the radius of the curvature of the silicon wafer before and after coating. The radius of curvature of the silicon wafer before and after deposition was measured using surface profilometry (Hommelwerke, Germany). All samples were measured in triplicate to get an average value.

The scratch test was conducted to determine the adhesion critical load between the coating and substrate. The instrument was equipped with a diamond indenter with a cone angle of 120° and tip radius of 0.2 mm. The sliding speed was 2 mm/min and the normal load was linearly increased from 0 N to 100 N at a rate of 50 N/min. The critical scratch load (L_c) was determined at the position where first spalling or flaking occurred as verified by SEM.

The tribological properties of the DLC coatings were determined using a ball-on-disk tribometer (HT-500, China) in a phosphate buffer saline (PBS, pH = 7.4) solution at room temperature (20 °C). The counterpart was an Al_2O_3 ball of 3 mm in diameter. The applied load of 3 N was kept constant at a fixed rotating frequency of 10 Hz. The friction was continuous until the DLC coatings were worn out as indicated by a sudden increase in the friction coefficient. The wear life was calculated by multiplying the frictional time with rotating frequency. Five measurements were conducted on each sample to get an average value.

1.3 Electrochemical corrosion measurements

The corrosion behavior of the DLC-coated and mirror polished NiTi alloy was evaluated in phosphate buffer saline (PBS, pH = 7.4) solution with an exposure area of 1 cm^2 at (37±0.5) °C by electrochemical impedance spectroscopy (EIS). All the electrodes were ultrasonically rinsed in acetone, alcohol, and distilled water for 15 min successively before measurements. The open circuit potential (OCP) of the electrode was continuously monitored for 120 min, starting immediately after immersion in the electrolyte and followed by EIS at OCP over a frequency range of 1 mHz to 100 kHz with a sinusoidal perturbation potential amplitude of 10 mV.

2 Results and Discussion

2.1 Coating characteristics

Fig.1 shows the Raman spectrum of the DLC coatings and the Gaussian fits. A wide peak between 1100 and 1800 cm^{-1} is distinct and can be deconvoluted into two peaks defined as *D* and *G*, respectively, which are the typical characteristic peaks of DLC coatings. The presence of a *D* peak centered at about 1350 cm^{-1} is ascribed to the breathing mode of sp^2 sites in the rings, whereas the G peak centered at about 1580 cm^{-1} is assigned to the stretching vibration of any pair of sp^2 sites in the chains or rings[13]. The variation in the DLC coating thickness with different deposition time and the fitted results are shown in Fig.2. The slope of the fitted line, i.e. the average deposition rate of DLC coatings, is 10.2 nm/min, which is comparable to that obtained by PECVD[14] and hybrid ion beam deposition[15]. According to the intercept of the fitted line at the film thickness axis (110.3 nm, i.e. the thickness of Ti interlayer) and deposition time of 5 min, the deposition rate of Ti interlayer is calculated to be 22.1 nm/min.

2.2 Mechanical properties

Fig.3 depicts the variation in the compressive stress and critical load of the DLC coatings as a function of film thickness. The residual compressive stress in the DLC coatings is around 4.5 GPa and decreases gently at a rate of 0.000478 GPa/nm as the film thickness increases and it is consistent with the results reported elsewhere[14-16]. R.K. Roy, et al ascribed it to the shift

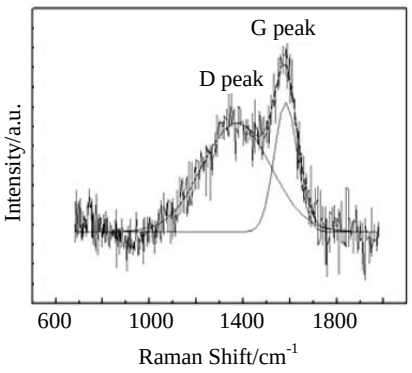

Fig.1 Raman spectrum of the DLC coatings and Gaussian fitting results

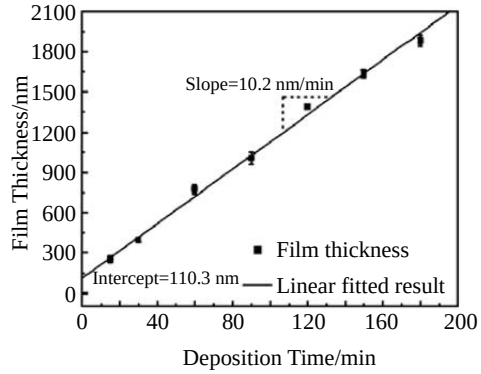

Fig.2 Thickness of the DLC coatings prepared within different deposition time

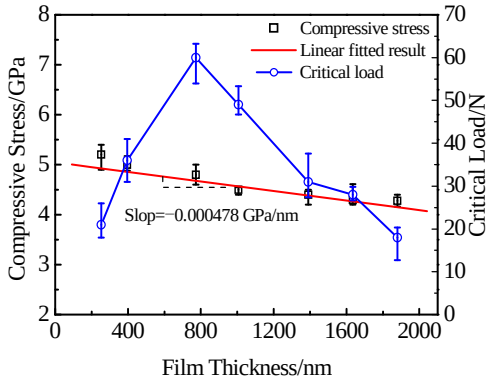

Fig.3 Variation of residual stress and critical load of DLC coatings as a function of film thickness

of the shear stress near the interface away from the coating-substrate interface with increasing coating thickness[15].

The scratch test is frequently used to evaluate the adhesion between coatings and substrates and is particularly valid for hard coatings on soft substrates[17]. In the present case involving hard DLC coatings on soft NiTi substrate, the measurement suffers from the normal force during scratching leading to plastic pile-up of the materials ahead of the indenter thus inducing bending and compressive stress in the coating. The bending stress σ_b is given by the following[18]:

$$\sigma_b = \frac{1.22E_f}{1-v_f^2}\left(\frac{t_f}{R_f}\right)^2 \quad (2)$$

where E_f and v_f are Young's modulus and Poission's ratio of the coating, t_f is the coating thickness, and R_f is the radius of the region of plastic pile-up. It is clear that as the film thickness increases, the critical bending stress increases. In this failure mode, semi-circular cracks extending to or beyond the edge of the scratch track are always observed. Under compressive stress ahead of the indenter, the critical stress value (σ_{cd}) for adhesive failure of the coating is the combination of the intrinsic compressive residual stress (σ_i) in the film and external compressive stress (σ_e) applied by the diamond indenter. σ_{cd} can be expressed as follows[19]:

$$\sigma_{cd} = \left(\frac{E_f\gamma_d}{t_f}\right)^{1/2} \quad (3)$$

where t_f is a given film thickness. It is clear that as the film thickness increases, σ_{cd} decreases. Since the difference in σ_i is minor for different film thickness as shown in Fig.3, a smaller σ_e, i.e. normal load, is needed to reach σ_{cd} as the film thickness increases. Flaking in or beyond the scratch track is often observed in this mode of failure. As shown in Fig.3, the critical load (L_c) of the coatings increases first and then decreases as the coating thickness increases. The L_c reaches about 60 N when the thickness of the coating is about 800 nm. Fig.4 shows the morphology of the scratch tracks and magnified images on samples with different film thickness. According to Fig.4a, the initial failure mode is manifested by semi-circular cracking without flaking, indicating it is a bending failure ahead of the indenter during scratching. As the film thickness increases, the critical bending stress increases as discussed previously and a larger normal load is needed to reach the critical bending stress. Consequently, the critical load increases. As shown in Fig.4g and the magnified image, flaking occurs at a small normal load, indicating the adhesive failure ahead of the indenter during scratching. As the film thickness increases, the critical compressive stress decreases as discussed above and a smaller normal load is needed to reach the critical compressive stress. Hence, the critical load decreases. Fig.4a and Fig.4b show the feature of bending failure whereas Fig.4e, Fig.4f and Fig.4g reveal the adhesive failure. Flaking becomes denser and wider as the film thickness increases. Therefore, as the thickness increases, a change in the failure mode from bending fracture to adhesive failure ahead of the

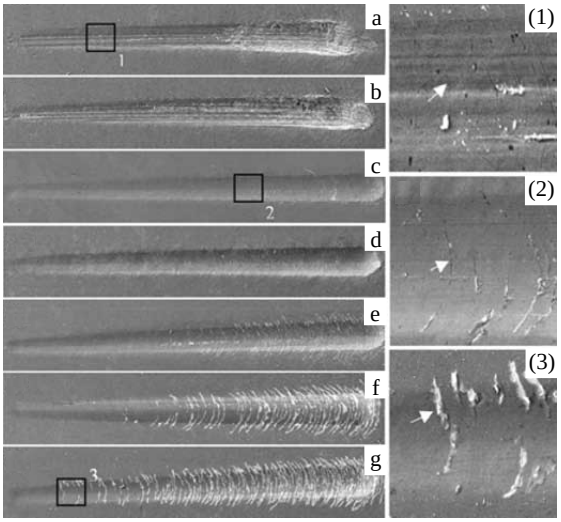

Fig.4 Scratch tracks on DLC coatings of different thickness: (a) 253 nm, (b) 426 nm, (c) 754 nm, (d) 1006 nm, (e) 1392 nm, (f) 1635 nm, and (g) 1880 nm. (1), (2) and (3) are the localized magnification of the rectangular zone in (a), (c) and (g) respectively

indenter can be distinguished. However, the stress field near the moving indenter is very complicated, and so usually the failure of the coating is due to a combination of bending and compressive stress.

Fig.5 presents the variation in the friction coefficient and wear life as a function of film thickness. The friction coefficient is approximately 0.08 regardless of film thickness. The origin of the low friction coefficient of DLC coatings has been investigated and it is mainly ascribed to the formation of a transfer film on the counterpart and graphitization of the coatings because of the friction-induced annealing at the contact regions[20]. For DLC coatings deposited with the same parameters (except deposition time) and tests conducted to evaluate the tribological performance under the same conditions, the wear mechanism and wear rate are assumed to be constant. The wear failure can be divided into two modes: progressive (abrasive, adhesive and diffusional) wear failure and catastrophic (spalling) wear failure depending on the magnitude and form of stress in the coating[21]. As the film thickness increases, the wear life increases linearly initially, indicating a constant wear rate and failure mechanism representative of progressive wear. However, when the film thickness exceeds 900 nm, the wear life of the coatings shows a small decrease indicating catastrophic wear failure after progressive wear for a certain time. Cheng and co-authors have also observed similar results from TiN coatings on Si_3N_4 substrates[21]. Another study concerning the wear life of DLC coatings on steel substrate also shows that for coatings with the same thickness, the wear life increases with higher adhesion strength[22], which may be due to that the transition from progressive wear to catastrophic wear is prolonged as the adhesion strength is increased.

2.3 Corrosion behavior

The Bode plots acquired from the uncoated NiTi alloy and those coated with DLC of different film thickness are presented in Fig.6. The impedances of the DLC-coated NiTi alloys are higher than that of the uncoated, as can be seen from Fig.6a. One capacitive behavior can be discerned from the uncoated NiTi alloy, while two capacitive behaviors are clearly observed from the DLC-coated samples irrespective of the film thickness. Based on the data, an equivalent circuit is proposed to model the EIS results of uncoated and DLC-coated NiTi samples (Fig.7). This method is commonly used to model the EIS results of porous and insulating polymer-coated metallic substrates[23]. The electronic elements in the equivalent circuit are described in the following. RE and WE correspond to reference electrode and the working electrode, respectively. R_s is the solution resistance of the electrolyte between the working and reference electrodes. R_{pore} corresponds to the resistance of ionic transfer across the micropores of the coating and R_p represents the inner layer resistance in the micropores or charge transfer resistance at the substrate/electrolyte interface. CPE_1 represents the inner layer

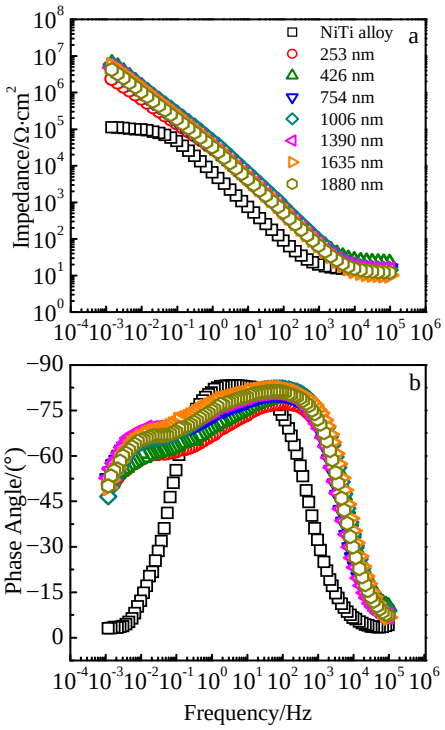

Fig.6 Bode plots of NiTi alloy of uncoated and coated with DLC prepared within different deposition time

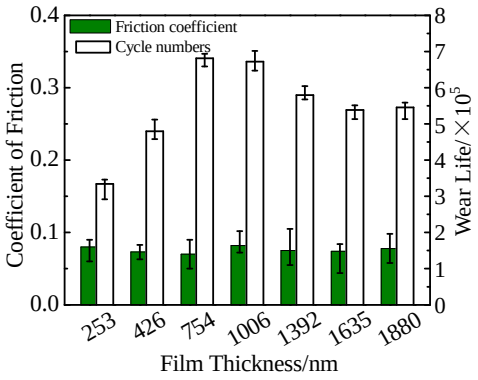

Fig.5 Variation of the friction coefficient and wear life of the DLC coatings as a function of film thickness

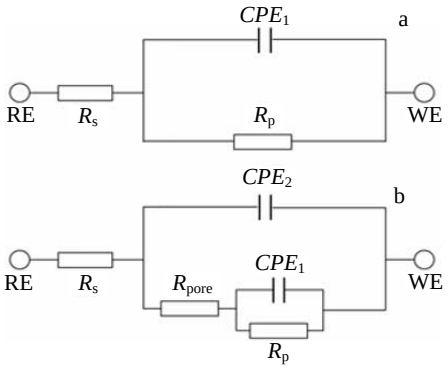

Fig.7 Equivalent circuit of uncoated (a) and DLC-coated (b) NiTi alloy

capacitance in the micropores or double layer capacitance at the substrate/electrolyte interface and CPE_2 corresponds to the capacitance of the DLC coatings. CPE_1 and CPE_2 are capacitances represented by the constant-phase elements (*CPE*). The impedance of *CPE* can be expressed as $Z_{CPE} = [Z_0 (j\omega)^n]^{-1}$, where Z_0 is the *CPE* constant, $j^2 = -1$ is the imaginary number, ω is the angular frequency, and n is the *CPE* exponent ($-1 \le n \le 1$)[24]. When n approaches to 1, the *CPE* can be seen as a non-ideal capacitor.

The results fitted according to the proposed equivalent circuits are shown in Fig.8. As shown in Fig.8a, the impedance values of the DLC-coated samples are higher than those of the uncoated one, indicating film protection. R_{pore} increases as the film thickness increases and the capacitance of DLC the coatings (CPE_2) shows the opposite trend compared to the impedance (R_{pore}). The capacitance of the DLC coatings (CPE_2) and resistance of the micropores (R_{pore}) can be expressed respectively as[25]:

$$CPE_2 = \varepsilon_0 \varepsilon_r (A/d) \quad (4)$$

and

$$R_{pore} = \rho (d/A_p) \quad (5)$$

where ε_0 is the dielectric constant of free space, ε_r is the dielectric constant of the DLC coatings, A is the exposed area of the working electrode, d is the coating thickness, ρ is the resistivity of the electrolyte, and A_p is the collective cross sectional area assuming that the mircopores in the film are perpendicular to the surface. According to Eqs. (4) and (5), as the film thickness increases [d in Eqs. (4) and (5)], CPE_2 decreases and R_{pore} increases linearly. Actually, as shown in Fig.8, CPE_2 and the film thickness bear a linear relationship approximately. With regard to R_{pore}, when the film thickness is less than 1300 nm, the linear relationship between the film thickness and R_{pore} is maintained, but when the thickness exceeds 1300 nm, R_{pore} only shows a small increase as the thickness goes up. In fact, as the film thickness increases [d in Eq. (4)], the diameter of the micropores near the coating surface, i.e. the collective cross sectional area [A_p in Eq. (5)] may increase thereby not obeying the linear relationship between R_{pore} and d. M. Yatsuzuka and co-authors also found the enlargement of micropores near the surface of DLC coatings using scanning probe microscope (SPM)[26]. As the film thickness increases, R_p increases initially and then stabilizes before dropping slightly finally. Its corresponding capacitance (CPE_1) exhibits a trend opposite to that of R_p. Usually, R_p corresponds to the inner layer resistance of the DLC coatings in the mircropores as indicated by the SPM image of the micropores in Ref.[26]. As the film thickness increases, the thickness of the inner DLC layer increases also, as indicated by the increased R_p and decreased CPE_1. However, when the thickness of the DLC coatings reaches about 400 nm, the inner layer thickness does not increase any more as indicated by the relatively steady values of R_p and CPE_1. From Fig.8b we can also deduce the inner layer of DLC coatings is inhomogeneous as indicated by the relatively small n value (n_1 of CPE_1) compared with that of outer layer (n_2 of CPE_2).

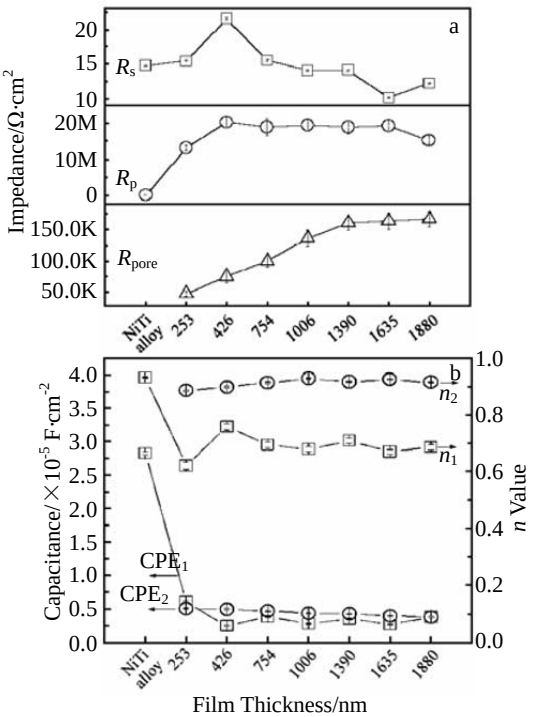

Fig.8 Fitted results of (a) impedance and (b) capacitance of uncoated NiTi alloy and DLC-coated NiTi produced using different deposition time

3 Conclusions

1) DLC coatings of thickness between 253 nm and 1880 nm can be deposited on NiTi alloy by arc enhanced magnetron sputtering. DLC coatings with film thickness between 700 nm and 1000 nm have favorable mechanical properties and corrosion resistance.

2) The residual compressive stress is about 4.5 GPa and decreases only slightly with larger film thickness, whereas the adhesion critical load increases initially and then decreases. A transition from bending failure to adhesive failure can be observed. The film thickness has no evident influence on the friction coefficient, but the wear life increases first and then decreases with the increase of the film thickness due to the transition in the wear mechanism from progressive wear failure to catastrophic wear failure.

3) The polarization resistance and pore resistance increase as the film thickness increases, but the increasing rate of both of them diminishes gradually.

References

1 Chu P K. *Nuclear Instruments and Methods in Physics Section B*[J], 2006, 242: 1

2 Imbeni V, Martini C, Prandstraller D *et al*. *Wear*[J], 2003, 254: 1299

3 Lu X Y, Bao X, Huang Y *et al*. *Biomaterials*[J], 2009, 30: 141

4 Poon R W Y, Yeung K W K, Liu X Y *et al*. *Biomaterials*[J], 2005, 26: 2265

5 Man H C, Ho K L, Cui Z D. *Surface and Coatings Technology*[J], 2006, 200: 4612

6 Grill A. *Diamond Related Materials*[J], 2003, 12: 166

7 Kobayashi S, Ohgoe Y, Ozeki K *et al*. *Diamond and Related Materials*[J], 2005, 14: 1094

8 Cai W, Sui J H. *Surface and Coatings Technology*[J], 2007, 201: 5194

9 Sui J H, Gao Z Y, Cai W *et al*. *Materials Science and Engineering A*[J], 2007, 454-455: 472

10 Zheng Y F, Liu X L, Zhang H F. *Surface and Coatings Technology*[J], 2008, 202: 3011

11 Hang R Q, Ma S L, Chu P K. *Diamond and Related Materials*[J], 2010, 19: 1230

12 Stoney G G. *Proceedings of the Royal Society of London. Series A*[J], 1909, 82: 172

13 Robertson J. *Materials Science and Engineering R*[J], 2002, 37: 129

14 Ohlídal I, Ohlídal M, Franta D *et al*. *Diamond and Related Materials*[J], 2005, 14: 1835

15 Roy R K, Ahmed S F, Yi J W *et al*. *Vacuum*[J], 2009, 83: 1179

16 Šniurevičiūtė M, Laurikaitienė J, Adlienė D *et al*. *Vacuum*[J], 2009, 83: s159

17 Bull S J, Berasetegui E G. *Tribology International*[J], 2006, 39: 99

18 Evans H E. *Materials at High Temperatures*[J], 1994, 12: 219

19 Donnet C, Erdemir A. *Tribology of Diamond-like Carbon Films: Fundamentals and Applications*[M]. New York: Springer, 2008: 115

20 Liu Y, Erdemir A, Meletis E I. *Surface and Coatings Technology*[J], 1996, 82: 48

21 Cheng H E, Hon M H. *Surface and Coatings Technology*[J], 1996, 81: 256

22 Chang C L, Wang D Y. *Diamond and Related Materials*[J], 2001, 10: 1528

23 Mansfield F. *Journal of Applied Electrochemistry*[J], 1995, 25: 187

24 Figueira N, Silva T M, Carmezim M J *et al*. *Electrochimica Acta*[J], 2009, 54: 921

25 Papakonstantinou P, Zhao J F, Richardot A *et al*. *Diamond and Related Materials*[J], 2002, 11: 1124

26 Yatsuzuka M, Tateiwa J, Uchida H. *Vacuum*[J], 2006, 80: 1351